

ULTRA AND VERY LIGHT DUCTED FAN PROPULSION SYSTEM COMPLEX DESIGN OPTIMIZATION

Daniel Hanus, Robert Theiner, Erik Ritschl

Department of Automotive and Aerospace Engineering, Faculty of Mechanical Engineering, Czech Technical University in Prague, Karlovo nam. 13, 121 35 Praha 2, Czech Republic

Keywords: *Light aircraft propulsion, ultra light ducted fan design, fan drive dynamics, piston engine installation and cooling, inlet channels external and internal aerodynamics*

Abstract

The propulsion system is being developed for the application to the full composite ultra-light two-seated airplane with maximum take off weight of 450 kg. The propulsion system consists of the piston engine of the power output of 150 HP at 10500 rpm, the composite fan driven by the lightweight aluminium alloy or composite shaft, the composite inlet channel and the composite jet nozzle with a by-pass cooling duct containing the engine radiators. The system is optimized to meet all airworthiness requirements for the VLA category with a minimum weight and maximum propulsive efficiency.

1 Introduction

A ducted fan propulsion system for UL and VL airplanes driven by piston engines enables considerably higher cruise speeds of the airplane, much better external aerodynamics, lower noise generation and safer ground operation in comparison with traditional propeller. In comparison with a pure hot jet propulsion by turbojet engines the operating cost is much lower and also the propulsive efficiency is considerably better. The airplane with ducted fan propulsion also offers the handling qualities of the jet plane. Moreover it can be used for a basic training of a jet pilot. The successful realization of the ducted fan propulsion system is however rather difficult. Many reported designs failed because of problems with fan efficiency and shorter life time due to vibrations excited by the flow field distortion at the inlet section of the fan. There

are also other problems including the internal and external aerodynamics of the inlet channel, complex design of the fan and its drive, the piston engine installation and mainly it's cooling. Finally, in the case of the engine failure the plane drag is increased by additional drag caused by the choked inlet.

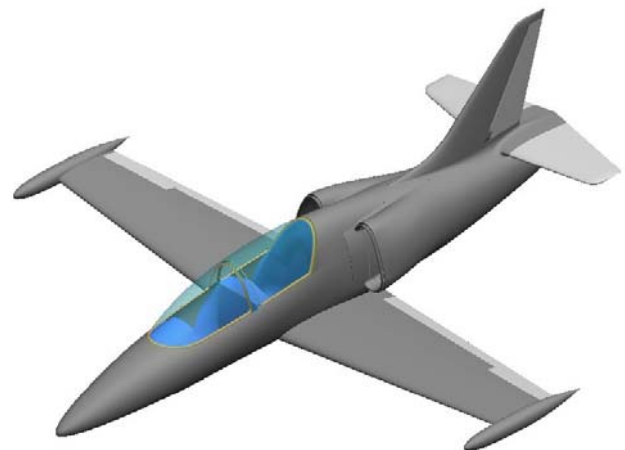


Fig. 1. Cold-jet UL39 ALBATROS with a ducted fan propulsion unit

UL – 39 ALBATROS characteristics

Span:	7.2 m (23.6 ft)
Length:	7.34 m (24.1 ft)
Height:	3.02 m (9.9 ft)
Wing area:	8.5 m ² (23.6 sq ft)
Empty weight:	280 kg (617.3 lb)
Max. TOW:	450 kg (992 lb)
V _{NE} :	285 km ph (177.1 m ph)
V _C (cruising sp.):	225 km ph (139.8 m ph)
V _{MIN} :	65 km ph (40.4 m ph)
Load factor:	+4; -2
Fuel consumption:	15 l ph (cruising sp.) (3.96 US gal ph)

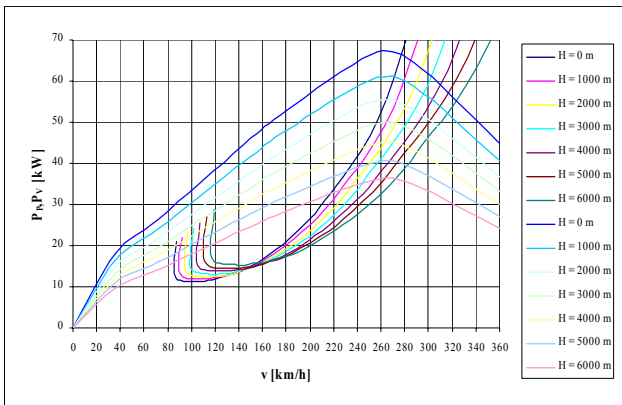


Fig. 2. Calculated airplane required power and the propulsion unit power altitude curves

2 Propulsion unit design characteristics

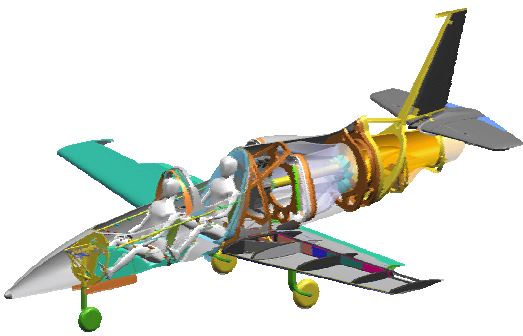


Fig. 3. UL propulsion unit installation concept

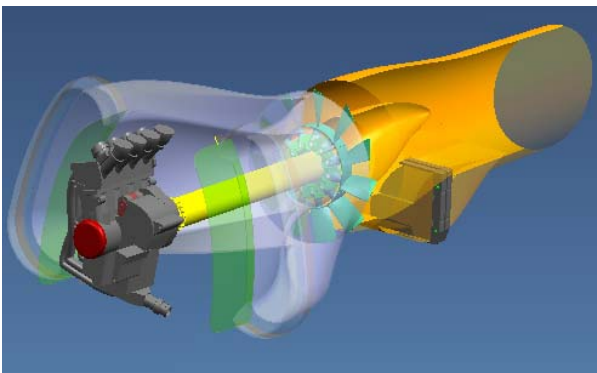


Fig. 4. Propulsion unit design concept

The propulsion unit consists of the piston engine driving by the transmission shaft the axial fan. The air from the atmosphere is induced through two fuselage intakes by the inlet channel. Compressed air by the fan is accelerated by the jet pipe. In the jet pipe two serial cooling radiators are placed into the special by-pass channel.

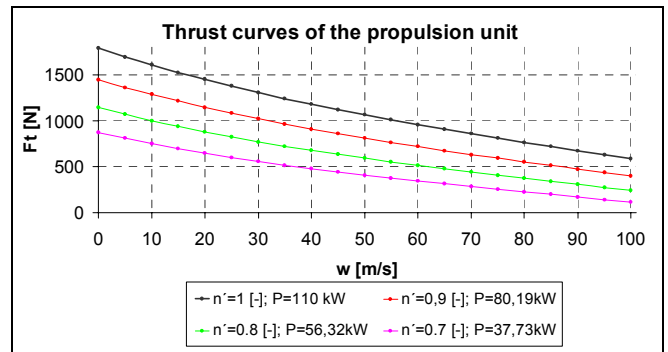


Fig. 5 Thrust curves of the designed propulsion unit

3 Inlet Channel

Inlet channel consists of two symmetric parts. The inlet channel leads the air from the external flow to the axial fan impeller. The channel has typical shape for the military jets with one jet engine installed in the fuselage of the airplane. It is very important to design the shape and position of the inlets and their leading edges as well as the overall shape of the internal duct to assure the stable internal flow with low pressure loss and the most possible uniform velocity distribution at the inlet plane of the fan rotor blades. This is necessary to provide the best possible flow conditions for stable operation of the fan and its highest possible efficiency at all flight operation regimes. The complex aerodynamic analysis based on the optimization of the geometry of the inlet channel using the CFD Fluent methods and 3D CAD Unigraphics led to the optimum shape of the channel. Special interest was devoted to calculations of the internal flows and boundary layer thickness development with the emphasis on the maintaining the laminar character of the boundary layer within the channel by the gradual acceleration of the flow. The overall curvature of the channels ducts were designed as smooth as possible with simultaneous acceleration of the flow to avoid excessive generation of contra rotating vortices the secondary flow pair. The friction losses depend on the state of boundary layer. The laminar boundary layer starts at the leading edge. The wall shear stress arises in boundary layer and is proportional to viscosity of the fluid (1).

$$\tau_L = \mu \frac{\partial w}{\partial y} ; \tau_T = \mu_T \frac{\partial w}{\partial y} \quad (1)$$

The transiting zone begins after certain

$$\tau_L = \mu \frac{\partial w}{\partial y} ; \tau_T = \mu_T \frac{\partial w}{\partial y} \quad (1)$$

The transiting zone begins after certain distance and later it starts changing to a turbulent boundary layer. The turbulent wall shear stress is described by similar equation like laminar (2). For the coefficient of turbulent viscosity μ_T is valid relation $\mu_T \gg \mu_L$ and the ratio μ_T / μ_L varies from 10^2 to 10^7 for different flow conditions. If the low energy lose inlet channel is requested than should be the laminar boundary layer kept as long as possible.

To decrease the growth of thickness of the laminar boundary layer it is possible by acceleration of outer velocity field. The controlling computation was made to predict the state of boundary layer at the end of inlet channel. The momentum thickness of laminar layer ν_2 is predicted for planar plate at distance 1m from the leading edge and flow velocity 50 m/s (3). The Reynolds number of laminar turbulent transition respecting the impact of the turbulent intensity of outer flow field is defined by the equation (4), where Tu is the intensity of turbulence in percents. Now is it possible to predict the intensity of turbulence in the inlet and outlet channel cross-sections. Computation

$\frac{\partial v}{\partial x}$	ν_2 [mm]	$\lambda * 10^{-8}$	Tu_1 [%]	Re_{ν_2}	ν [mm]
0.54	0.194	1.392	0.34	790	0.231
0.40	0.218	1.302	0.28	839	0.245
0.26	0.256	1.322	0.24	923	0.270
0.12	0.300	0.740	0.19	1070	0.312
0.00	0.363	0.000	0.16	1255	0.366
-0.14	0.415	1.651	0.11	1501	0.438

Tab 1

using these input data was made for: stream velocity $w_1=50$ m/s, pressure $p_1=101\ 325$ Pa and temperature $T=288$ K. Turbulence intensity in inlet face was computed using the equation (5)

with prediction that the fluctuation components are independent on the ratio $\partial v / \partial x$. The results are presented in Tab. 1.

$$\nu_2 = \frac{1}{8} \delta_L ; \quad (3)$$

$$\delta_L = 5,2 \sqrt{\frac{\nu^* x}{w_{00}}} = 5,2 \frac{x}{\sqrt{Re_x}}$$

$$Re_{\nu} = 402 * Tu^{-0,6} \quad (4)$$

$$Tu_1 = Tu_2 \frac{w_2}{w_1} \quad (5)$$

$\frac{\partial v}{\partial x}$	w_2 [m/s]	ν_2 [mm]	Tu_2 [%]	Tu_1 [%]
0.54	77.00	0.194	0.22	0.34
0.40	70.00	0.218	0.20	0.28
0.26	63.00	0.256	0.19	0.24
0.12	56.00	0.300	0.17	0.19
0.00	50.00	0.363	0.15	0.15
-0.14	43.00	0.415	0.13	0.11

Tab.2

If the flow is accelerated, boundary layer sensitivity to turbulence intensity decreases [2].

State of boundary layer in channel is described by Reynolds number of laminar layer momentum thickness (6) and it depends on pressure gradient parameter λ (7).

$$Re_{\nu} = 402 * Tu^{-0,6} \left[1 - \exp(-Tu) \frac{1 - \exp(-40 * \lambda)}{1 + 0,4 \exp(-40 * \lambda)} \right] \quad (6)$$

$$\lambda = \frac{\nu^2}{\nu} * \frac{\partial w}{\partial x} \quad (7)$$

The solution results are displayed in following table Tab. 2. There are the values of parameter λ and for this values computed Reynolds numbers. Value of impulse thickness is valid for beginning of transition of the boundary layer.

Previous calculation indicates that the transition of boundary layer should occur at

higher turbulence intensity number and in longer distance from leading edge.

The Shape of the inlet channel was designed with aim to maintain the laminar boundary layer all along the channels length, so the ratio $\partial v / \partial x$ is kept on the value 0.54 for each designed variant. Different geometry varies only in inlet cross sections shapes and position against the outlet face. Many different variant were made through the design process.

Aerodynamic quality of the designed geometry was tested by CFD method. The boundary condition was set to a value of velocity inlet 50 m/s at the inlet cross-section. Pressure outlet was set at the outlet cross-section. In the part of the channel where both halves are joined was set symmetry boundary condition. The model of turbulence was chosen the k-ε and the turbulence intensity was set to the value of 0.2 %. The velocity field of final variant of inlet channel is shown below on the Fig. 6. It is valid for designed regime. The velocity field of outlet face is almost uniform.

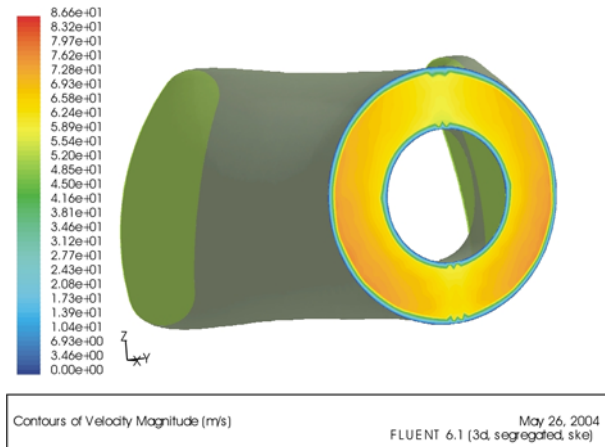


Fig. 6. Velocity field at the outlet section of the inlet channel at designed operation mode

The velocity varies from main velocity about eight percent

4 Fuselage Aerodynamics

As the designed airplane operates at significant lower speeds than real jet, the orientation and position of the inlet orifices are designed to assure perfect function at the whole range of the engine and airplane operation states. It is necessary to prove also the case of the failure of

the engine and its influence to the drag of the inlet channel orifices with very low mass air flow. This has been simulated by the worst case with zero mass air flow through the channel. Various different shape variants of the intake orifices and their position and orientation were studied and external flow fields and the drag of the inlet were calculated with the aim to find the best geometry assuring the minimum drag increment in the case of the failure of the engine. Next figures show the results of these calculations for two different inlet shapes, first for the protuberant intakes at the Fig. 7 and then for the backwards inclined intakes. It is evident that the protuberant intake induces more disturbances in the external flow field and more important drug increment when the flow through the channel is blocked than the backwards inclined one [3].

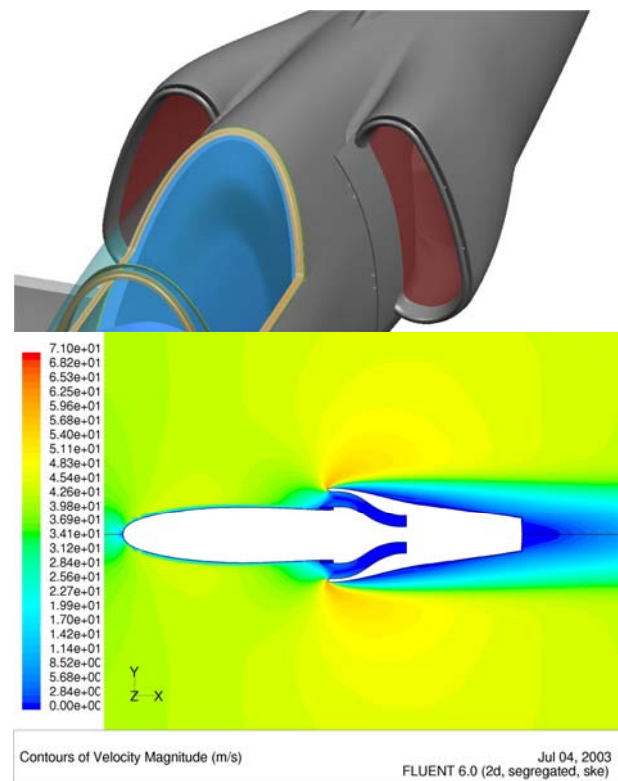


Fig. 7. External velocity field of the fuselage with the protuberant intakes and zero internal flow in the inlet channel

The CFD calculations discover large area of separated flow behind the inlet lips, Fig. 7. This can be very dangerous for the flight control. The design compromise led to the skewed inlet lips.

The calculations of the external flow fields are based on the airplane CAD model created by Unigraphics CAD system. The geometrical model of the airplane is placed into the space of the computation area. The area is divided into two parts as shown in figure 8. The inner area is limited by the negative impression of the fuselage surface.

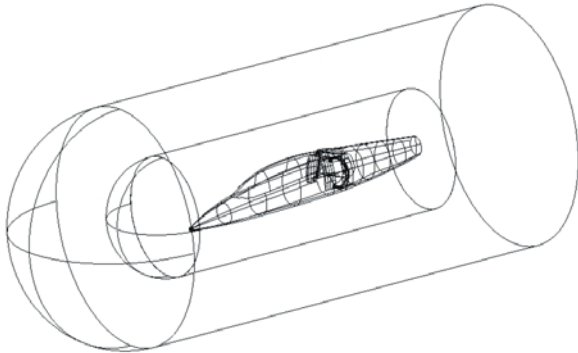


Fig. 8. Scheme of the computation area

Dimensions of area are following: airplane fuselage length of 7.34 m, inner area length of 9.5 m the outer diameter of 3m. Outer area has the length of 15 m and outer diameter the length of 6 m.

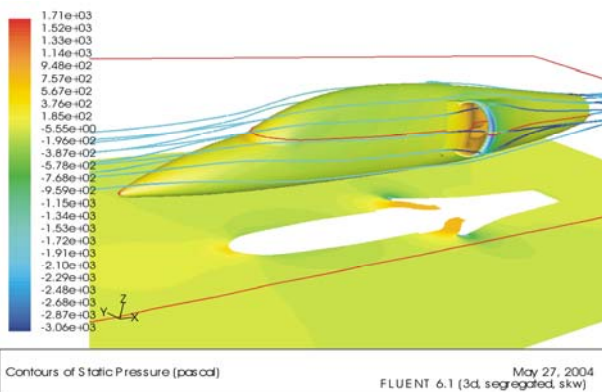


Fig. 9. Calculated static pressure distribution in the flow field around the fuselage with zero mass flow through the inlet channel at flight velocity $v = 40$ m/s

The computation mesh was generated by using software Gambit. Airplane surface was meshed by triangular elements, spacing size from 10 to 50.

The volume of mesh size increases as the distance from the airplane surface up to value 300 in the outer region surface. The T-grid scheme was used to mesh the volume. Computation of flow field around the airplane

was made by using solver Fluent 6. The flow description was set to the incompressible viscous flow with $k-\epsilon$ turbulence model.

The turbulence intensity of the free stream was set to the value of 0.5 % at the inlet plane. During the analysis process different flight conditions were tested. The case of the engine failure was computed as the worst possible flight condition. The boundary conditions were following: The velocity of flight $w = 40$ m/s as the inlet velocity used on the forward and side surface of computational area and the wall condition was selected at the fan impeller inlet plane. On the other hand the case with running fan was tested at the same flight velocity. The boundary condition in the rotor inlet plane was set to get the atmospheric pressure (0 Pa) at the outlet of the jet pipe, so the gauge pressure of -3840 Pa and backflow turbulence 10%. In all flight conditions the outlet pressure at the exit plane of the region was set to the atmospheric pressure, so the gauge pressure is 0 Pa.

The computed results are shown on the figure 9. This is the worst case with stopped engine and zero mass flow through the inlet channel. In the bottom of the figure there is shown the 2D distribution of the static pressure in the cross section highlighted by orange lines. On the picture the separated flow on the outer side of leading edge of the intake lips is visible. The streamlines as well as the overall static pressure distribution on the fuselage indicate that the external flow is not seriously affected and that the additional drag is rather small.

The second calculated flight case is represented by normal function of the propulsion unit and the results of the calculations are shown on the figure 10.

For both two cases the drag of the fuselage was calculated. The relative increase of the drag caused by choked inlet channel was 33 % of the value calculated for the normal operating propulsion unit.

Another verification of the inlet channel aerodynamic qualities has been made considering the take off operating regime. The flight velocity was set to zero. On the figure 11 the velocity field on the plane at the fan rotor

and also the static pressure distribution on the wall of the inlet channel are shown. The velocity varies from 58 to 78 m/s, average velocity is 63.5 m/s. The velocity field is almost uniform and provides sufficient fan operating conditions.



Fig. 10. Calculated static pressure distribution in the flow field around the fuselage with running engine at flight velocity $v = 40$ m/s

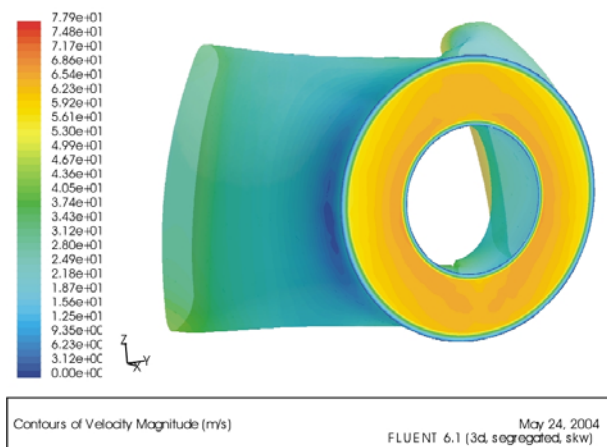


Fig. 11. Pressure distribution on the surface of the inlet channel and the velocity distribution at the exit plane at zero flight velocity

5 Fan stage design

Design parameters of the fan at sea level:

The air mass flow: $m = 18.39 \text{ kg}\cdot\text{s}^{-1}$

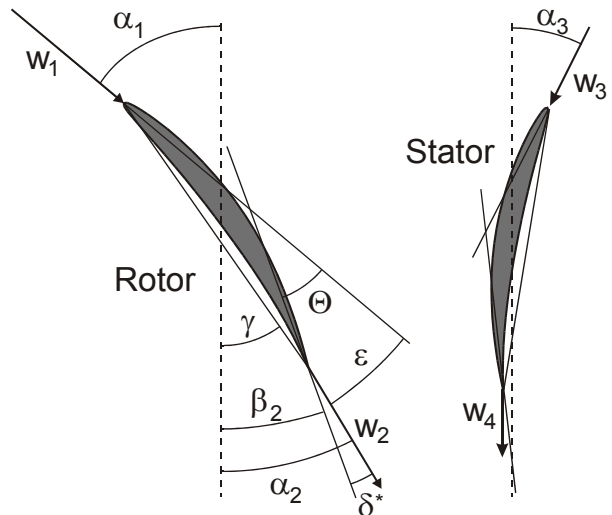
Root radius: $r_{\text{root}} = 150 \text{ mm}$

Tip radius: $r_{\text{tip}} = 290 \text{ mm}$

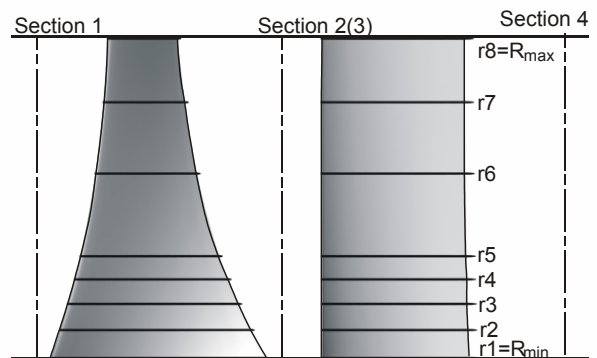
RPM: 6200 revolutions per minute

Pressure ratio: $\pi_{\text{fan}} = p_{4\text{tot}} / p_{1\text{tot}} = 1.0648$

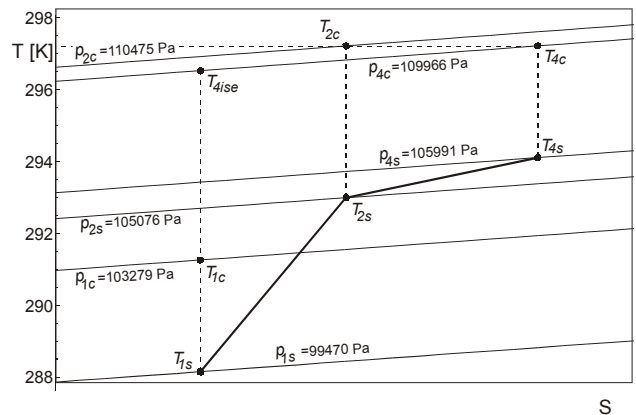
Isentropic efficiency of the fan: $\eta_{\text{fan}} = 0.885$



Rotor blade and stator vane geometry parameters



The axial flow passage of the fan computed flow surfaces



Computed thermodynamic states of the air within the fan and the chart of the compression on the cylindrical flow surface of the fan stage at the radius r_7 in the entropy diagram

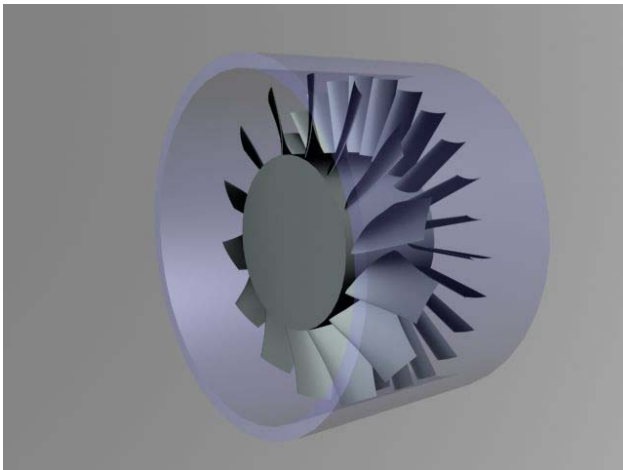


Fig. 12. Aerodynamic design of the rotor blades and stator vanes configuration of the fan

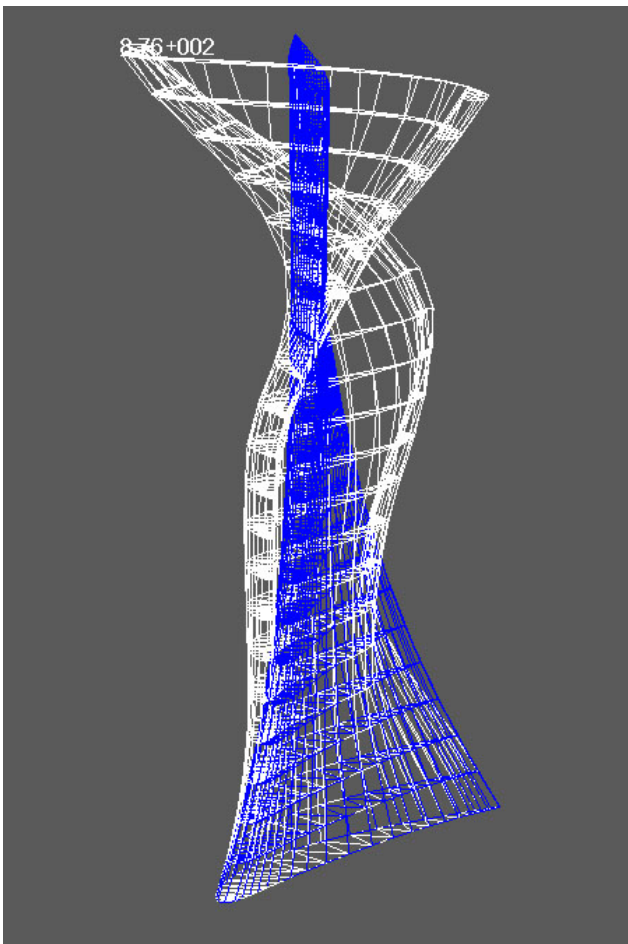


Fig. 13. The fan blade mode 4 dynamic analysis Composite skin and foam core design

The stress and dynamic analysis of the composite blade in the operation at whole range of the engine ratings up to the maximum RPM proved mechanical resistance and safety of the design fan blades.

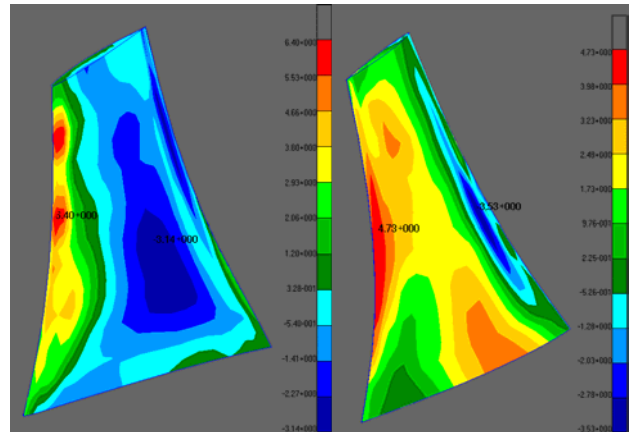


Fig. 14. Tensions at longitudinal and transversal directions in the surface layer of the composite fan blade at the take-off engine rating

6 Engine installation and cooling

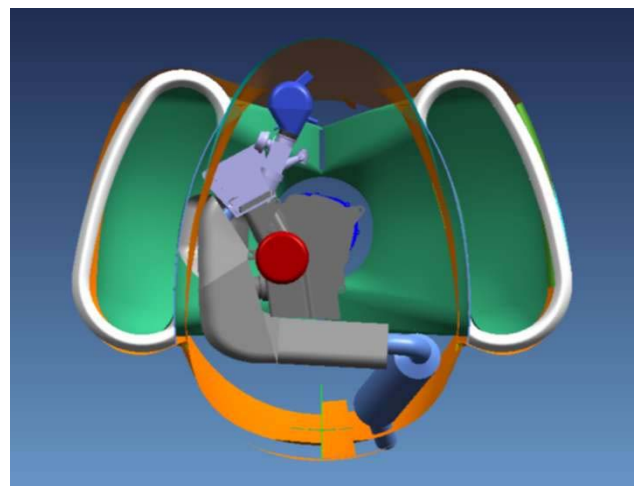


Fig. 15. Piston engine installation - cross section

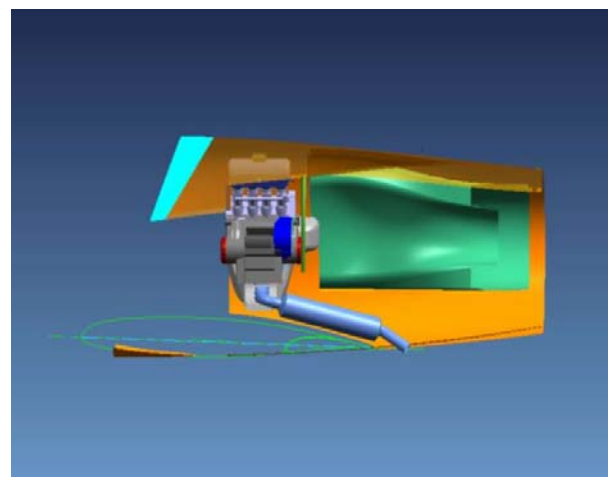


Fig. 16. Piston engine installation - longitudinal section

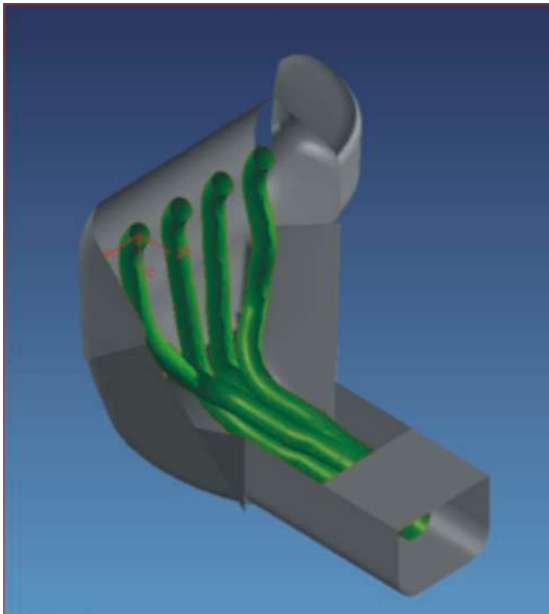


Fig. 17. Exhaust manifold cooling casing



Fig. 18. Inlet channel with two slots (in red) for ventilation of the engine space by the suction

The engine internal space ventilation air mass flow: $m_{vent} = 0.125 \text{ m}^3/\text{s}$

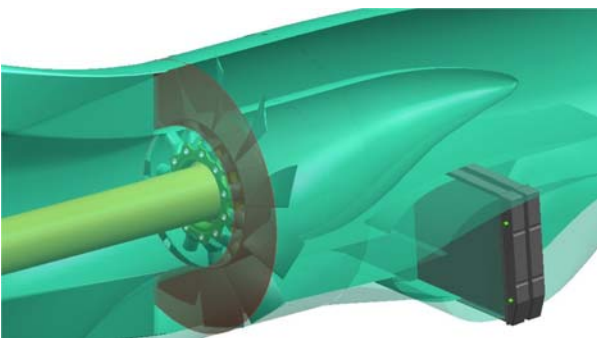


Fig. 19. Front part of the jet pipe with the by-pass cooling channel and radiator

Diameters of the inlet annulus of the jet pipe:
Hub: 300 mm, Shroud: 580 mm, Inlet velocity of the air: 80 m/s.

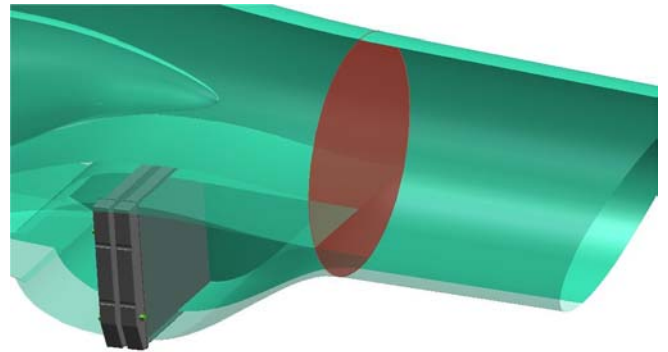


Fig. 20. Rear part of the jet pipe with the by-pass cooling channel and cooling radiators

Jet pipe outlet diameter:

$$D_{\text{Jet pipe out.}} = 440 \text{ mm}$$

Jet pipe outlet air velocity:

$$V_{\text{Jet pipe out.}} = 102 \text{ m/s}$$

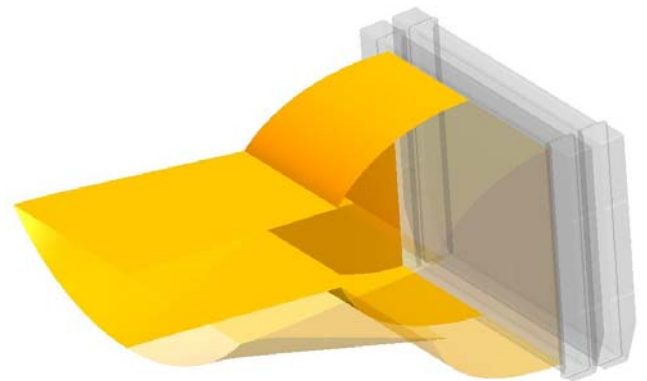


Fig. 21. Front part of the by-pass cooling channel with inlet diffuser and two serial cooling radiators

The radiators inlet cross section dimensions:

Width: 295 mm, Height: 266 mm

Inlet velocity of the cooling air: 25 m/s



Fig. 22. Rear part of the by-pass cooling channel with the outlet accelerating nozzle



Fig. 23. Assembly of the jet pipe with the cooling channel

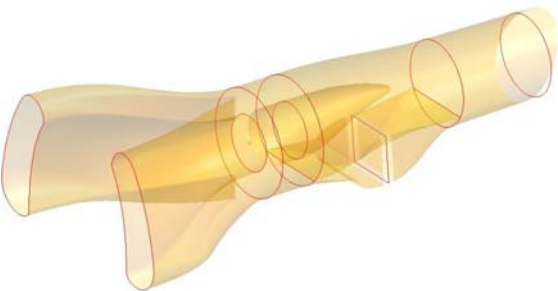


Fig. 24. The overall propulsion unit flow passage

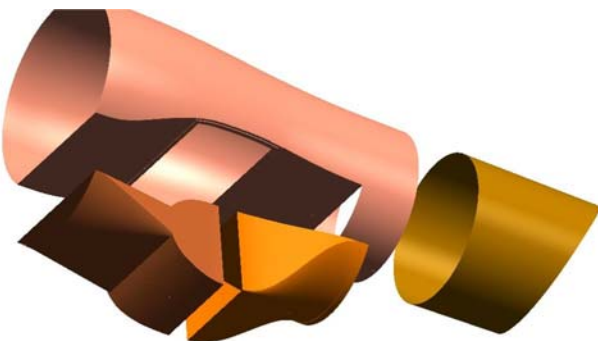


Fig. 25. Principal parts of the jet pipe made of composite materials

Designed maximum cooling performance of the both radiators at maximum engine rating is 110 kW.

7 The fan drive dynamics



Fig. 26. Transmission shaft manufactured of the high strength aluminium alloy

The rotor system is being developed to satisfy functional, weight, stiffness and stability requirements and dynamic behaviour at a range of operational speeds. The main part of the rotor is a high-strength light alloy hollow shaft (995 mm length, 1 mm shell thickness, 116 mm diameter). Very important and difficult technological problems were solved and experimentally proved.

The primary reduction gear ratio of 1:1.581 reduces 10500 RPM of the engine to 6640 RPM of the fan driving shaft. The torsional shakings of the piston engine are dumped efficiently by two soft rubber joints. The soft rubber joints of the transmission shaft of the fan drive serving at the same time as clutches are designed to assure supercritical torsional operation at whole range of the engine ratings.

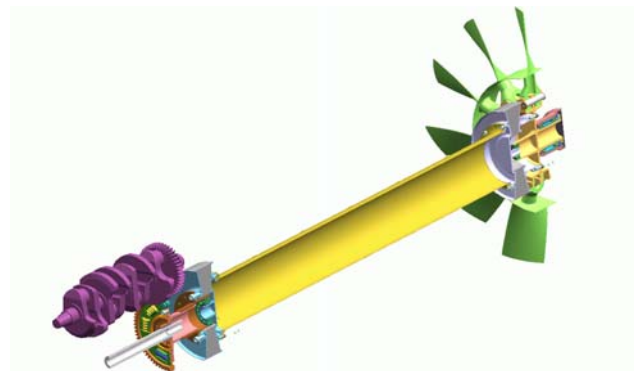


Fig. 27. Assembly of the fan drive with the reduction gear, front rubber joint, lightweight hollow drive shaft, rear rubber joint and the fan disk with the roll bearing

8 Conclusion

The feasibility study of ultra-light ducted fan propulsion unit driven by a motorcycle piston engine was made. The propulsion unit design is applied for the propulsion of a fully composite ultra-light airplane specially designed as a replica of the jet trainer Aero Vodochody L 39 Albatros. This application leads only to the above described design concept with the fuselage intakes, rather long inlet channel and so with the necessity to have also considerably long transmission shaft of the fan drive with the engine placed in front of the inlet channel. This

concept is very challenging and brings number of different design problems to be solved. First, aerodynamic design of the inlet channel and the fan was made, then the strength and the dynamics of the fan drive was verified and third the engine installation was solved in a number of alternatives and then calculated the engine cooling system. The design process was really complex taking in account at first the best possible aerodynamic and operational performance characteristics of the unit and its main parts, strength, mechanical and dynamic reliability and safety. The individual modules of the system were optimized with the aim to get the most lightweight possible construction. In the design process the 3D CAD system UNIGRAPHICS was used in the combination with CFD software FLUENT and also other finite elements computational methods for calculation stresses at the individual parts and their dynamic behaviour by NASTRAN and PATRAN software. The chosen composite materials and progressive manufacturing technology allows reach minimum weight of the propulsion unit.

In the table 3 calculated weights of the propulsion unit are given.

Part of the propulsion unit	Weight in kg
Inlet channel	10.5
Jet pipe	5.5
Piston engine of the power output 110 kW with accessories	60,0
Engine mount	8,0
Fan	8,0
Fan drive	3.0
Whole propulsion unit assembly: MPU	94,0

Tab. 3. Weights of the propulsion unit parts

Maximum static thrust: $F_{\max} = 1751 \text{ N}$

The static thrust to propulsion unit weight ratio: $F_{\max} / \text{MPU.g} = 1.9$

The thrust of the propulsion system at maximum speed of flight: $F_{\text{TVmax}} = 800 \text{ N}$.

The propulsive efficiency of the propulsion system at maximum speed of flight 80 m.s^{-1} (288 km ph) is: $\eta_{\text{propulsive}} = 0.66$.

The total efficiency of the propulsion system (considering the fan efficiency) is: $\eta_{\text{tot prop}} = 0.58$.

Acknowledgement

This research was carried out in the Aerospace Research Centre supported by the Czech Ministry of Education, Sports and Youth, by grant No LN 00B 051 and as a part of the project supported by grant No J04/98:212 2 00009.

References

- [1] J. Jerie, *Elementare Theorie der Doppelwirbel in Gekrummten Kanalen*, Wiss. Zeit. d. TU Dresden, 37, 1988, 87-93
- [2] B. Thwaites, *Approximate Calculations of the Laminar Boundary Layer*, Aero Quart., 1, 1949, 245-280
- [3] F. Marc de Piolenc, G. E. Wright Jr., *Ducted fan design*, Vol. 1, Mass flow, 1997, 61-86
- [4] D. Gay, *Matériaux composites*, Hermes, 1997
- [5] B. C. Hoskins, A.A.Baker, *Composite Materials for Aircraft Structures*, American Institute of Aeronautics and Astronautics, Inc., 1986
- [6] K. Potter, *Resin Transfer Moulding*, Chapman & Hall, 1997
- [7] D. Hanus, *Inlet and Outlet Casings of the Turbojet Engines-Design and Experiment*, Acta Polytechnica, Journal of Advanced Engineering Design, Vol. 40 No.4/2000, pp. 101-109, ISSN 1210-2709, Publishing House of the CTU in Prague, 2000
- [8] O. Uher, *Mathematical Modeling of Behavior of Filament Wound Composite Structures*, CTU in Prague, 2002
- [9] D. Hanus, E. Ritschl, R. Theiner, *Inlet Channel for a Ducted Fan Propulsion System of a Light Aircraft*, Acta Polytechnica, Jurnal for Advanced Engineering Design, vol. 43, no. 6, s. 3-8. ISSN 1210-2709, Publishing House of the CTU in Prague, 2003